Long RT-PCR of the entire 8.5-kb NF1 open reading frame and mutation detection on agarose gels.

J M Martinez, H H Breidenbach and R Cawthon

Genome Res. 1996 6: 58-66
Access the most recent version at doi:10.1101/gr.6.1.58

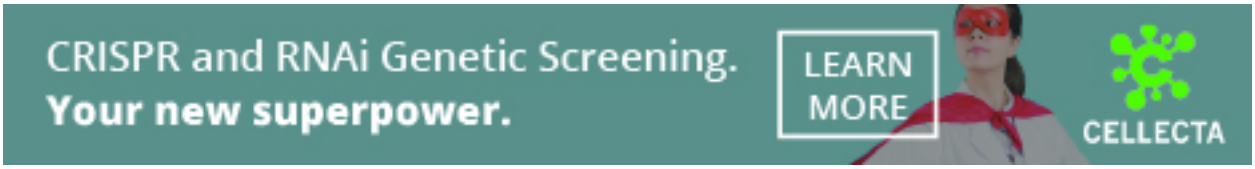

GENOME METHODS

Long RT–PCR of the Entire 8.5-kb *NF1* Open Reading Frame and Mutation Detection on Agarose Gels

Jennifer M. Martinez,[1] Heidi Huntsman Breidenbach,[1] and Richard Cawthon[1–3]

[1]Department of Human Genetics, [2]Huntsman Cancer Institute, University of Utah, Salt Lake City, Utah 84112

Previous approaches to mutation detection in mRNA from the neurofibromatosis 1 (*NF1*) locus have required the PCR amplification of five or more overlapping cDNA segments to screen the entire 8.5-kb open reading frame (ORF). Systematically, these assays do not detect deletions that span the region of overlap (usually 1–3 exons) of any two consecutive target segments. In such cases, amplification from the mutant region of the disease-causing allele fails because binding sites for the PCR primers are missing, but amplification from the normal allele proceeds, yielding only the normal product. To alleviate this problem, we have developed a protocol to reverse transcribe and amplify the entire protein-coding sequence of *NF1* as a single PCR product, starting with total RNA from lymphoblast cell lines or from whole blood. The 8.7-kb RT–PCR product was prepared from nine NF1 patients with known deletions or insertions, ranging in size from a 30-bp deletion within 1 exon to a 2.4-kb deletion that removes 12 exons. Agarose gel analysis of the initial products detected deletions as small as 341 bp. Restriction endonuclease digestion with *Ase*I and *Fsp*I, followed by agarose gel electrophoresis, revealed the predicted abnormal bands in all nine patients. All mutant bands were identified readily by observers with no knowledge of the patients' mutations. This simple assay should detect a great variety of insertion/deletion mutations in the *NF1*mRNA internal to the primer binding sites, including all possible single and multiple exon dropouts and ~30% of all previously reported *NF1* mutations.

Neurofibromatosis 1 (NF1) is a hereditary disorder that typically gives rise to flat hyperpigmented spots on the skin (cafe-au-lait spots), and benign tumors along peripheral nerves (neurofibromas) and in the iris (Lisch nodules) (Riccardi 1992). NF1 patients also are at increased risk for developing certain cancers (Blatt et al. 1986; Riccardi and Eichner 1986; Sorensen et al. 1986). With an incidence of ~1 in 3500 in both sexes and in all racial/ethnic groups, NF1 is the most common hereditary disease predisposing to malignancy. Whereas germ-line mutations in the *NF1* gene cause NF1, somatic *NF1* mutations in the general population appear to contribute to the development of various cancers (Li et al. 1992; Andersen et al. 1993; The et al. 1993).

The *NF1* gene occupies ~350 kb of genomic DNA at *q11.2* in chromosome 17 (Li et al. 1995). The gene has 60 known exons; alternative splicing includes or excludes exons 9A (Danglot et al. 1995), 23A (Nishi et al. 1991), and 48A (Cawthon et al. 1990). The *NF1* mRNA is 11–13 kb (Viskochil et al. 1990; Wallace et al. 1990); recently, an additional normal polyadenylated *NF1* transcript containing only exons 1–10c was described (Takahashi et al. 1994). The smallest *NF1* exon, 9A, is 30 bp; the largest exon, 16, is 441 bp (Li et al. 1995).

Rapid, comprehensive screening for inactivating mutations in large genes is a difficult task. When mRNA is available from the mutant allele of the gene of interest, as is the case for nearly all patients with NF1 (Hoffmeyer et al. 1995; R. Cawthon, unpubl.), screening is simplified. There have been many reports of screening sets of unrelated NF1 patients for mutations in the *NF1* gene by various methods. The report achieving the highest rate of mutation detection so far is also the only one in which the entire protein-coding region of the gene was screened (Heim et al. 1995). These investigators, applying the protein truncation test (PTT) (Sarkar and Sommer 1989; Powell et al. 1993; Roest et al. 1993), transcribed and translated five overlapping RT–PCR products spanning the *NF1* open reading frame

[3]Corresponding author.
E-MAIL cawthon@genetics.utah.edu; FAX (801) 585-3833.

6:58–66 ©1996 by Cold Spring Harbor Laboratory Press ISSN 1054-9803/96 $5.00

(ORF) and identifed mutations in 14 of 21 NF1 patients (67%). A similar detection rate in NF1 patients was obtained with the PTT in our own laboratory (H. Breidenbach, unpubl.)

Because of limitations in translating large proteins in vitro and in resolving large proteins on polyacrylamide gels, PTT currently has an upper limit of ~2 kb for the largest PCR product that can be screened effectively. Therefore, the 8.5-kb ORF of *NF1* must be divided into overlapping segments for amplification. This limitation means that deletion mutations large enough to span the entire region of overlap of two consecutive cDNA segments that are the targets for amplification will prevent amplification from the mutant allele, and these mutations will be missed.

Recently, modified reaction conditions that allow PCR amplification of much longer DNA targets were described (Barnes 1994; Cheng et al. 1994). Long RT–PCR of the entire *NF1* ORF followed by agarose gel electrophoresis, presented here, allows identification of a great variety of large deletions that would be missed in smaller, overlapping RT–PCR products. Furthermore, small insertion/deletion mutations present in many of the patients that show apparently normal long RT–PCR products can be detected conveniently by digestion of the long RT–PCR product with *Ase*I and *Fsp*I, followed by agarose gel electrophoresis.

RESULTS

Figure 1 summarizes our strategy for mutation detection in long RT–PCR products from *NF1*. Total RNA from Epstein–Barr virus (EBV)-transformed lymphoblasts or from whole blood was the template for RT–PCR. Previous work has shown that these cells express both the (+) 23A and the (–) 23A forms of the *NF1* transcript, but do not express either (+) 9A or (+) 48A transcripts. Therefore, the long RT–PCR method presented here should amplify, from control individuals, only *NF1* (–) 9A (+) 23A (–) 48A (8754 bp) and *NF1* (–) 9A (–) 23A (–) 48A (8691 bp).

Reverse transcription is primed with a specific antisense oligonucleotide downstream of the *NF1* stop codon. PCR from the resulting cDNA is then performed using a pair of primers flanking the ORF. The product of this long RT–PCR is screened for deletions and insertions by agarose gel electrophoresis. To allow detection of smaller deletions and insertions and to narrow the location of all detected mutations, the long product is then digested with restriction endonucleases that release a set of fragments with unique sizes that are well separated by agarose gel electrophoresis. The restriction fragments predicted for an *Ase*I–*Fsp*I double digest (using the Site Program from the Intelligenetics Suite) appeared suitable for this purpose and are shown in Figure 1.

To test its effectiveness, we applied this approach to mutation detection to all of the patients in our NF1 collection with known deletions or insertions 30 bp or longer that fall entirely between exons 1 and 49 of the *NF1* gene. The mutations in *NF1* mRNA of the nine patients constituting this set have not been reported previously; their sizes and locations are shown in Figure 1 and Table 1. Table 1 also lists the observed and expected sizes of the mutant bands before and after restriction digestion, and the normal restriction fragments affected by the mutations.

Figure 2 shows the results of gel electrophoresis in 0.8% agarose of long *NF1* RT–PCR products prepared from the nine NF1 patients and three controls. A band of ~8.7 kb was shared by all samples. Because the (+) and (–) 23A forms of *NF1* differ in length by only 63 bp, resolution of the mixed RT–PCR products into two bands (8754 and 8691 bp, respectively) is not expected under these conditions. Agarose gel electrophoresis of long *NF1* RT–PCR product prepared from whole blood RNA of a control gave results equivalent to those shown in the control lanes in Figure 2.

Figure 3 shows the patient samples and a control after double digestion with *Ase*I and *Fsp*I and additional electrophoresis in a 1.5% agarose gel until the bromophenol blue had migrated nearly to the bottom of the gel (19 cm). The six restriction fragments expected from normal *NF1* RT–PCR products were observed in all samples. The largest two fragments, Ia and Ib, appeared to have a size difference consistent with alternative splicing of the 63-bp exon 23A. [All restriction digest data presented here were obtained using *Fsp*I and *Ase*I. However, we now recommend that *Fsp*I be replaced by the isoschizomer *Avi*II (see Methods)].

One of the difficulties of mutation detection in RNA samples from NF1 individuals arises from the fact that 80% of patients show unequal levels of mRNA from the two *NF1* alleles (Hoffmeyer et al. 1995). In two-thirds of the patients tested, the abundance of mRNA from one *NF1* allele was more than twice that of the other allele. That study used heterozygosity at a single-base-pair

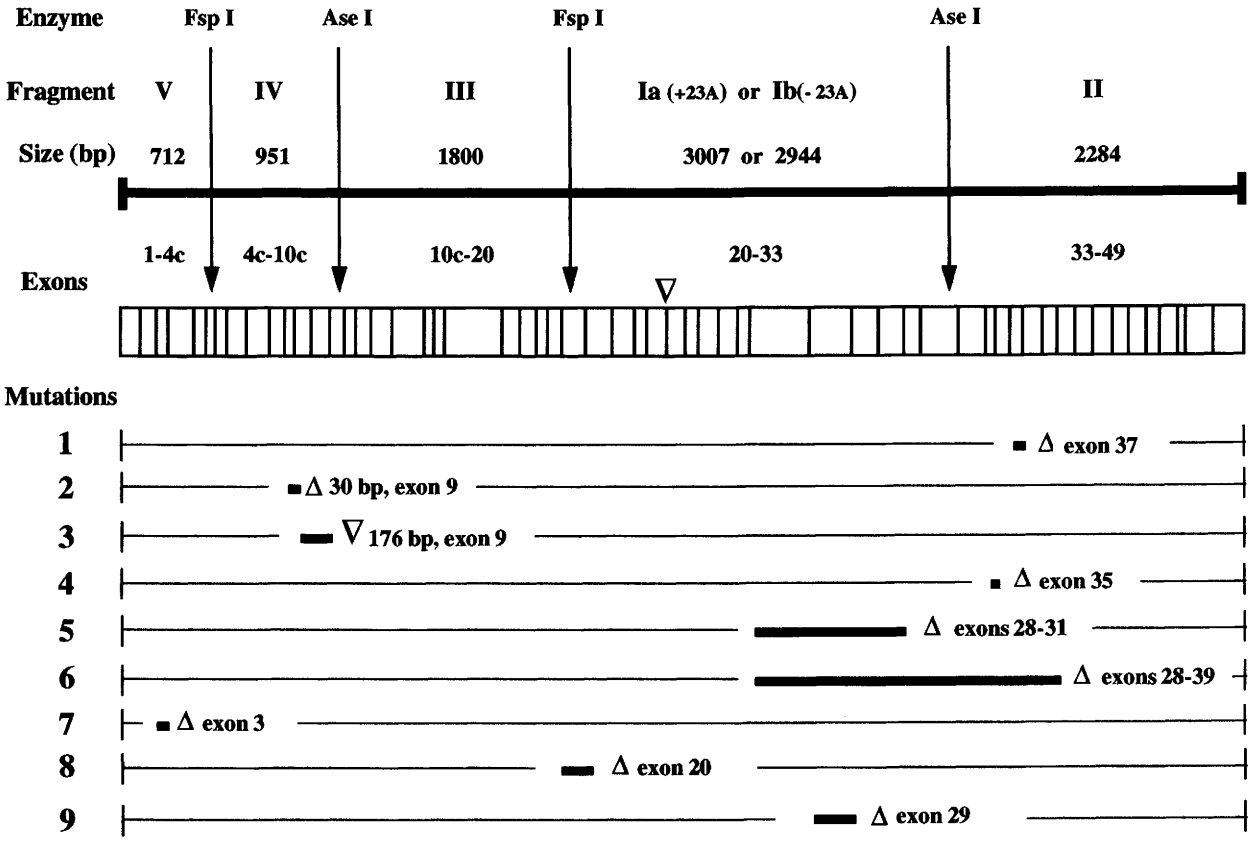

Figure 1 Long *NF1* RT–PCR product. Maps of *AseI–FspI* restriction sites, *NF1* exons, and patients' mutations. (*Top*) The solid horizontal bar represents the 8.7-kb *NF1* RT–PCR product. Positions cut by the restriction endonucleases are indicated by downward-pointing arrows. The open horizontal bar just below the arrowheads contains vertical bars marking the boundaries between exons. There are 57 exons shown, which are numbered consecutively 1–49, with exon 4 split into exons 4a, 4b, and 4c; exon 10 split into exons 10a, 10b, and 10c; exon 12 split into exons 12a and 12b; exon 19 split into exons 19a and 19b; exon 23 split into exon 23-1 and 23-2; and exon 27 split into exons 27a and 27b. In addition, the alternatively spliced exon 23A is represented by the open arrowhead just above the exon 23-2/exon 24 junction. Exons 9A and 48A are not included because they are not expressed in lymphoblasts. (*Bottom*) The NF1 patient mutations used to validate the assay. (*Left*) They are numbered according to the gel lanes containing them in Figs. 2 and 3. (△) A deletion; (▽) an insertion.

polymorphism (bp 702 in the *NF1* ORF) to distinguish RT–PCR products from the two alleles. In our studies of *NF1* RT–PCR products, whenever unequal levels of mRNA have been detected, the mutant mRNA has proven to be the less abundant one. Therefore, it was not surprising to find that several of the mutant bands obtained after restriction digestion of the long *NF1* RT–PCR products (Fig. 3, asterisks) are more diminished in intensity, relative to the corresponding normal bands, than can be accounted for by their molecular weight differences.

Four independent operators, ignorant of the particular mutations present in this patient set, were given printed images of the gel shown in Figure 3, marked only as to which lanes contained NF1 patient samples and which contained the control sample. Each operator quickly found the mutant band(s) for each patient.

Mutations Detectable on Agarose Gels Prior to Restriction Enzyme Digestion

Patients 11573 and 11360

Electrophoresis of the initial, uncut long RT–PCR products (Fig. 2) until the product from controls had migrated ~2.5 cm from the origin allowed identification of two mutations: a 1.1-kb deletion in patient 11573 (lane 5), and a 2.3-kb deletion in patient 11360 (lane 6). The size of each deletion was calculated by subtracting the observed size of

Table 1. NF1 Patients, Their Known Mutations, and Mutant Band Sizes Determined by Agarose Gel Electrophoresis Before and After Restriction Digestion with *AseI–FspI*

Lane no.	Patient no.	Mutation	Size of mutant band by AGE: observed (predicted)[a]	Restriction fragment affected	Size of mutant band by AGE after restriction digest: observed (predicted)[a]
1	11387	del exon 37 (102 bp)	—	II	2189 (2182)
2	119-01	del 30 bp from exon 9	—	IV	918 (921)
3	11389	ins 176 bp into exon 9	—	IV	1126 (1127)
4	12359	del exon 35 (62 bp)	—	II	2229 (2222)
5	11573	del exons 28–31 (1171 bp)	7578 (7583 + 23A; 7520, –23A)	Ia, Ib	1840 (1836, + 23A; 1773, –23A)
6	11360	del exons 28–39 (2354 bp)	6390 (6400, +23A; 6337, –23A)	Ia, Ib, II	2880 (2937, +23A; 2874, –23A)
7	11344	del exon 3 (84 bp)	—	V	627 (628)
8	107-06	del exon 20 (182 bp)	—	Ia, Ib, III	4604 (4625, +23A; 4562, –23A)
9	94-04	del 148 bp from exon 29	—	Ia	2865 (2859, +23A)
				Ib	2802 (2796, –23A)
9	94-04	del exon 29 (341 bp)	8439 (8413, +23A; 8350, –23A)	Ia	2682 (2666, +23A)
				Ib	2624 (2603, –23A)

[a]Sizes of the observed mutant bands are given. The numbers in parentheses to the right of the observed sizes are the sizes predicted based on previous independent analyses of the mutations. (AGE) Agarose gel electrophoresis. Band sizes were determined with the FragmeNT Analysis Program (Molecular Dynamics, Inc.).

the mutant band (Table 1) from the average size for the normal (±) 23A RT–PCR products (8723 bp). The approximate location of these deletions within the long RT–PCR product can be deduced from the sizes of the abnormal fragments generated by restriction enzyme digestion (Fig. 3). In patient 11573, deletion of a single 1.1-kb segment from the *AseI–FspI* restriction map in Figure 1 could produce the 1.8-kb mutant fragment observed after restriction digestion (Fig. 3, lane 5) only if the deletion falls within fragment I. Similarly, in patient 11360, a 2.3-kb deletion could produce the 2.9-kb mutant fragment observed after restriction digestion (Fig. 3, lane 6) only if the deletion takes out the *Ase*I site at the fragment I/fragment II boundary.

Previous work has shown that the mutation in patient 11573 is a deletion of 11 kb of genomic DNA removing exons 28–31, and the mutation in patient 11360 is a deletion of 40 kb of genomic DNA removing exons 28–39 (Viskochil et al. 1990; R. Weiss, GenBank accession no. LO3723). In both cases, because the deleted regions are well away from the region of exon 23A, both the (+) and (–) 23A forms of *NF1* mRNA are expected to be synthesized from the mutant alleles. Because of the small size of the length differences, resolution of the (+) and (–) 23A mutant bands by gel electrophoresis prior to restriction digestion was not expected. After restriction digestion, however, two mutant fragments 63 bp apart were expected from each of these two patients. Only a single mutant restriction fragment from each patient was observed (Fig. 3). It is likely that the lower mutant band from patient 11573 did not resolve from the normal 1800-bp band and that the higher mutant band from patient 11360 did not resolve from the normal 3007-bp band.

Patient 94–04

Continued agarose gel electrophoresis of the initial, uncut long RT–PCR products until the full-length control products had migrated 8.5 cm from the origin revealed one additional abnor-

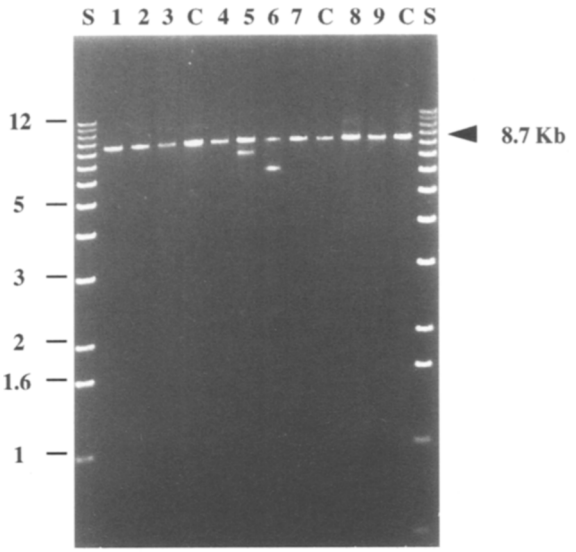

Figure 2 Agarose gel electrophoresis of long *NF1* RT–PCR products. (S) 1-kb standard ladders (GIBCO–BRL); (C) non-NF1 controls. Lanes *1–9* correspond to mutations 1–9 in Fig. 1. (Lane *1*) Patient 11387; (lane *2*) patient 119-01; (lane *3*) patient 11389; (lane *4*) patient 12359; (lane *5*) patient 11573; (lane *6*) patient 11360; (lane *7*) patient 11344; (lane *8*) patient 107-06; (lane *9*) patient 94-04. The band shared by all the samples was estimated to be 8716-bp by the Molecular Dynamics FragmeNT Analysis Program. The two normal *NF1* RT–PCR products (± the alternative exon 23A) are predicted to have an average size of 8723 bp.

mal band of ~ 8.4 kb, in patient 94-04 (data not shown). This corresponds to a deletion size of ~300 bp. Restriction digestion and additional agarose gel electrophoresis revealed four mutant bands in this patient (Fig. 3, lane 9), ranging in size from 2.6 to 2.9 kb. Removal of a continuous stretch of 300 bp from the *Ase*I–*Fsp*I restriction map (Fig. 1) will produce a restriction fragment in the size range of the observed mutant bands only if the removed stretch falls within fragment I.

Furthermore, if the deletion in fragment I does not involve the exon 23A region, it should yield double mutant bands 63 bp apart, one from the (+) 23A splice form and the other from the (–) 23A splice form. Size analysis of the four mutant bands revealed that the size difference between the two smallest mutant bands approximated the size of exon 23A, as did the size difference between the two largest mutant bands. The simplest interpretation of these results is that the mutation of this patient results in two distinct mutant versions of *NF1* mRNA with deletions of different size, both lying within fragment I and neither affecting the (±) 23A alternative splicing. Only the larger deletion is detectable by agarose gel electrophoresis of the uncut long RT–PCR product. Analysis of the results shown in Figure 3 indicates that the deletions are ~323 and 142 bp. Additional PCR-based experiments have demonstrated that both deletions lie between the primer 5′GCTCTCAAGCTAGCTCACAA-3′ in exon 28 and the primer 5′-GCACACAGAAGATTATAGGCA-3′ in exon 30; the larger deletion removes exactly exon 29 (341 bp) (H. Breidenbach and R. Cawthon, unpubl.).

Mutations Detectable Only After Restriction Enzyme Digestion

The mutations of the remaining six patients were undetectable prior to restriction enzyme diges-

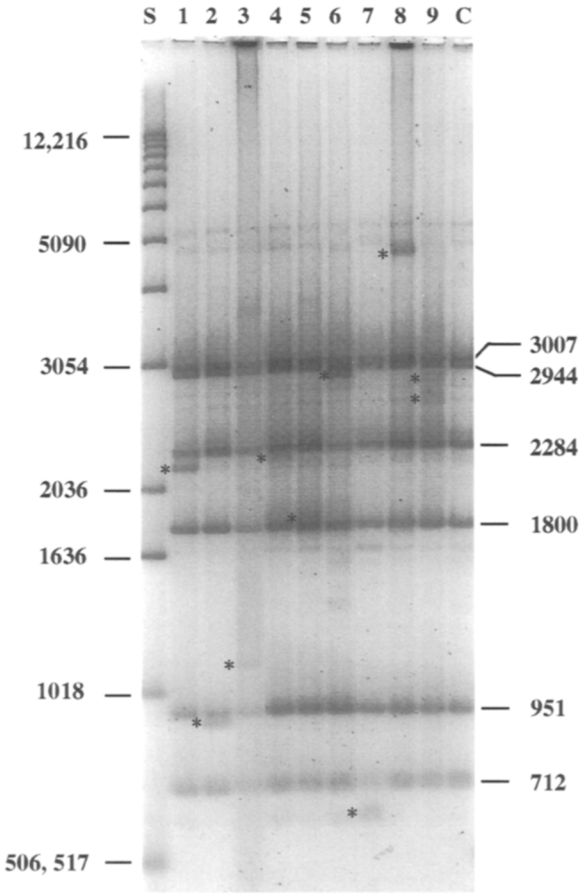

Figure 3 Agarose gel electrophoresis of long *NF1* RT–PCR products digested with *Ase*I and *Fsp*I. (S) 1-kb standard ladder (GIBCO–BRL); (C) non-NF1 control. (Lanes *1–9*) The order of patients is the same as in Figs. 1 and 2. An asterisk is placed immediately to the *left* of each mutant band.

tion. Insertion/deletion mutations undetected by agarose gel electrophoresis of the uncut long *NF1* RT–PCR product should be <300 bp. Therefore, in these patients the mutant fragments resulting from the *Ase*I–*Fsp*I digestion usually will migrate in proximity to the corresponding normal restriction fragment, allowing easy approximate localization within the *NF1* ORF. This prediction was upheld for five of the six patients (Fig. 3; Table 1).

Exceptions to this rule include any small mutation that removes one of the restriction sites targeted for *Ase*I–*Fsp*I digestion, thereby generating a disproportionately large mutant restriction fragment. The approximate location of such mutations often can be deduced from the size of the resulting fragments. For example, a deletion of <300 bp from the *NF1* long RT–PCR product will result in a mutant fragment ~4.6 kb after restriction digestion (Fig. 3, lane 8) only if it removes the *Fsp*I restriction site in exon 20. Sequencing of small RT–PCR products spanning the exon 20 region of this patient, 107-6, has demonstrated that the mutant *NF1* mRNA is missing exactly the sequence of exon 20.

The approximate location of a mutation also can be deduced when the loss of signal intensity from the position of one or more of the normal restriction fragments, relative to the signal intensity of the other normal fragments in the same lane, is large enough to measure. The signal decrease occurs because the mutant fragment shifts in the gel lane away from the position(s) of the normal fragment(s). Examples of this are the mutations in patients 11360 and 11344. With the unaided eye, it is clear in Figure 3 that fragment II (lane 6) and fragment V (lane 7) are diminished relative to the other normal-sized fragments in the same lanes. Less obvious signal losses from normal fragments, resulting from other mutations, were identifiable on careful quantitation with Molecular Dynamics ImageQuaNT software. However, this approach will not succeed in all cases, because of the very low abundance of some patients' mutant *NF1* mRNAs.

DISCUSSION

Long RT–PCR of the entire *NF1* ORF and analysis of the products on agarose gels before and after restriction digestion with *Ase*I and *Fsp*I is shown here to be a highly effective way to identify a great variety of *NF1* mutations. In the assay reported here, for all nine patient samples analyzed, the mutant bands observed on agarose gels before and after restriction digestion were the sizes predicted based on the patients' known insertion/deletion mutations. The greatest strength of the assay is its power to yield mutant RT–PCR products from deletion mutations that would be missed by traditional methods. For example, both of the deletions in patients 11573 and 11360 would not be detected by the protein truncation assay described by Heim et al. (1995), because the binding sites are removed for both the downstream primer of the S3 segment and the upstream primer of the S4 segment.

The power of gel electrophoresis to resolve bands of similar size depends in part on the location of the bands relative to the electrophoretic front during electrophoresis (R_f = distance of band from the origin/distance of the electrophoretic front from the origin); the best resolution is an R_f near 0.5. Because the 2% difference in length between the normal fragments Ia and Ib was resolvable at an R_f of ~0.31, it is likely that the smallest possible single exon dropout from lymphoblast *NF1* mRNA, the 47-bp exon 47, would be detected also: It contributes 2.1% of the length of fragment II, which has an R_f of ~0.36 in these 1.5% agarose gels.

These considerations also suggest that a few samples with no apparent abnormalities by a single gel analysis of the *Ase*I–*Fsp*I digestion products may reveal small deletions or insertions upon re-electrophoresis of the samples on two additional gels, one with a lower agarose concentration to optimize resolution of fragments Ia, Ib, II, and III, and the other with a higher agarose concentration to optimize resolution for of IV and V.

Occasionally, mutant restriction fragments will be missed when they are of low intensity and indistinguishable in size from one of the faint background bands appearing in all samples. Because the sizes of several of these faint bands are determined by the positions of the recognition sites for the restriction enzymes, this problem may be solved by use of a second set of restriction enzymes to cut the long *NF1* RT–PCR product, in place of the *Ase*I–*Fsp*I combination.

The assay presented here should detect ~30% of the mutations reported to date to the NF1 Mutation Consortium (Korf 1995). Currently, we are in the process of testing its detection rate in a set of unrelated NF1 patients. Expressed as mutations identified per *NF1* RT–PCR product, this assay should far surpass all assays reported previously. It will be particularly useful in the detec-

tion of large deletions removing multiple *NF1* exons. The principles of long RT–PCR and restriction analysis for mutation detection applied here to the *NF1* gene will be applicable equally to any large gene where scattered inactivating mutations predominate and mutant mRNA is accessible.

METHODS

RNA Isolation and cDNA Synthesis

EBV-transformed lymphoblastoid cell lines from NFI were grown in RPMI-1640 with 15% fetal bovine serum in a humidified incubator in the presence of 5% carbon dioxide. Total RNA from lymphoblastoid cells was isolated using TRI-Reagent (Molecular Research Center, Inc., Cincinnati, OH) according to the manufacturer's instructions. Whole blood was obtained by venipuncture from a non-NF1 control, with isocitrate as the anticoagulant. Total RNA was prepared directly from 3 ml of blood using the PURE*script* RNA Isolation Kit from Gentra Systems, Inc. (Minneapolis, MN), according to the manufacturer's instructions. The yield was 18 μg of total RNA, as determined by spectrophotometry.

Reverse transcription was performed using 400 units of the reverse transcriptase SuperScript II (GIBCO–BRL) and 10 μg of total RNA specifically primed with 0.2 pmole of the antisense oligonucleotide DV352 (5′-CCCACTTTCTTTGCAGTTGTTCTG-3′) in a final volume of 40 μl, according to the manufacturer's instructions, except for the following modifications. Thirty units of RNasin (Promega) was mixed with the oligonucleotide primer prior to addition of the RNA sample. A drop of mineral oil was then added to minimize evaporation during the incubations. After heating and chilling to anneal the primer to the RNA, the mixture of 5 × first strand buffer, DTT, and dNTPs was added as recommended, but with the addition of another 30 units of RNasin. Following the addition of SuperScript II, the samples were incubated at 42°C for 1 hr, then at 70°C for 15 min. After cooling on ice, 4 units of ribonuclease H (GIBCO–BRL) was added, followed by incubation at 37°C for 20 min. The cDNA synthesis buffer was then exchanged with 10 mM Tris, 0.1 mM EDTA, using a Centricon-100 concentrator (Amicon), with negligible change in sample volume. The use of only 2 μg of RNA in the above cDNA synthesis procedure occasionally resulted in a complete failure to amplify from one of the two NF1 alleles during the subsequent PCR step.

Long PCR

A pair of PCR primers flanking the NF1 ORF was selected, with the requirements that the primers would be long enough to allow two-temperature cycling during the PCR and be unlikely to prime extension on copies of themselves, on the other primer, or from any site in the accumulating PCR product internal to the correct primer-binding sites. Using the FindPatterns program of the GCG suite (Wisconsin Package 1994) with parameters set to default, we generated a list of alignments of candidate primers with NF1 cDNA sequence (both sense and antisense directions), allowing the total number of mismatches to be ≤10. Then, for a given candidate primer we checked whether the sequence of the last 4 bases at the 3′ end of the primer perfectly matched the aligned sequence for any of the alignments listed for that primer, and we rejected all candidate primers that showed one or more perfect matches of this type. The first primer pair to pass this test was the sense strand oligonucleotide SS5N5 (5′-CCTCACCTCAGCCTCCGCTCCC-3′) and the antisense oligonucleotide SS3N4 (5′-ATCTGGCAACATGGCAAACCGGATG-3′). The 5′-terminal base of SS5N5 corresponds to the 89th base upstream of the *NF1* initiating methionine codon. The 5′-terminal base of SS3N4 corresponds to the 145th base downstream of the *NF1* STOP codon.

In both primers phosphorothioate linkages were introduced in place of the last two phosphodiester linkages at the 3′ end to enhance the specificity of the primers and block the 3′ exonuclease activity of *Vent* polymerase (Noronha 1992; Skerra 1992). We have not tested whether the same primers with standard phosphodiester linkages throughout would yield equally good results.

PCR amplification from first-strand cDNA was performed using the Perkin Elmer GeneAmp XL PCR system in a final volume of 40 μl containing 1× XL buffer: 0.2 mM dNTPs, 0.4 μM of each primer, 0.25 mM spermidine, 1.1 mM $Mg(OAc)_2$, 8 μl of cDNA, and 1.2 units of rTth DNA Polymerase XL (contains *Vent* DNA polymerase also). PCR reactions were performed in Perkin Elmer MicroAmp reaction tubes in a Perkin Elmer 9600 thermal cycler. All reactions were initiated by a hot-start procedure. Reaction mixture were prepared in a volume of 32 μl each, containing 0.5 × XL PCR buffer and all other reagents, except the DNA polymerases. The reaction mixture were then covered with a drop of mineral oil. Next, the tubes were covered with the full plate rubber cover and the heated lid. The samples were heated at 93°C for 1 min, then brought to an 80°C holding temperature. The heated lid and full plate cover were then removed. The DNA polymerase mixture was delivered in an 8 μl volume containing 3 × XL PCR buffer, and the full plate cover and lid were replaced. The holding temperature was then released and cycling proceeded as follows: 93°C, 15 sec, 68°C, 12 min for 17 cycles; then 93°C, 15 sec, 68°C, 12 min plus 15 sec autoextension period per cycle for 12 cycles; followed by a 10-min extension at 70°C, and an indefinite holding temperature of 4°C. (Yield and specificity both declined when all reagents were mixed prior to the first denaturation. Thus, a hot-start step is mandatory for optimal results.)

Note: Perkin Elmer states in the package insert for its GeneAmp XL PCR Kit that the XL buffer contains tricine, potassium acetate, glycerol, and DMSO; however, the exact concentrations of these reagents are not given, as that information is proprietary. Furthermore, the original XL buffer from Perkin Elmer, used in the experiments reported here, has been replaced recently by XL buffer II in all new kits and XL DNA polymerase samples shipped. The exact composition of XL buffer II is also proprietary and unavailable. Perkin Elmer promises to continue to make the original XL buffer available to all investigators who request it. We have not tested yet whether replacing the original XL buffer with XL buffer II in our protocol yields equally good results.

Restriction Enzyme Digest and Analysis

For each RT–PCR product, the PCR buffer was exchanged with water using a Centricon-100 concentrator. Five microliters of the 8.7-kb PCR product and λ *Hin*dIII mass standards was analyzed on 1 × Tris-acetate–EDTA (TAE) 0.8% agarose gels containing ethidium bromide and photographed with transillumination by UV light. Between 200 and 870 ng (~20 μl) of each sample was then digested with 10–20 units *Fsp*I (New England Biolabs) under mineral oil in a final aqueous volume of 50 μl containing 50 mM Tris-HCl (pH 8.0) and 10 mM $MgCl_2$, at 37°C for 4 hr. The enzyme was then heat inactivated at 68°C for 20 min. Between 10 and 20 units of *Ase*I (New England Biolabs) and additional reagents were then added to a final volume of 70 μl containing the following: 50 mM Tris-HCl (pH 8.0), 10 mM $MgCl_2$, 100 mM NaCl, and 1 mM DTT. Incubation was then carried out at 37°C for 4 hr, followed by heat inactivation at 68°C for 20 min. After consecutive digestion with *Fsp*I and *Ase*I, the sample was concentrated by Centricon-100 centrifugation and/or evaporative centrifugation in a Savant Speed-Vac and analyzed on a 20-cm 1 × TAE 1.5% agarose gel until the bromophenol dye front had traveled nearly the length of the gel. Following electrophoresis, the gel was stained with a 1:10,000 dilution of stock Sybr Green I nucleic acid gel stain (Molecular Probes, Inc.) in 1 × TAE for 15 min and scanned using a FluorImager (Molecular Dynamics) with the 530 DF30 yellow filter in place.

The data in Figure 3 were obtained using the procedure described above for double digestion of the *NF1* RT–PCR product. Recently, however, we were successful in greatly simplifying the protocol for restriction digestion. *Avi*II (Boehringer-Mannheim) is an isoschizomer of *Fsp*I that has a recommended buffer for digestion that is identical to that of *Ase*I (New England Biolabs). We therefore replaced *Fsp*I with *Avi*II, and found that we could digest the *NF1* long RT–PCR product simultaneously with a mixture of *Avi*II and *Ase*I. In our current protocol, upon completing the long PCR step, 100–200 ng of PCR product (10–20 μl) was diluted directly into a final volume of 25–30 μl containing 1 × *Ase*I buffer (New England Biolabs), 4 mM spermidine, 1 mM DTT, and 10 units each of *Avi*II and *Ase*I. Incubation was done at 37°C for 1 hr. The digestion products were then analyzed by agarose gel electrophoresis as described above.

Estimation of Band Sizes on Agarose Gels

All length determinations of gel bands were performed using the Molecular Dynamics Fragment Analysis software, version 1.1, running under Microsoft Windows NT on an Intel 486-based computer. The point-to-point logarithmic option for size analysis was applied. The size standard was the GIBCO–BRL 1-kb ladder.

ACKNOWLEDGMENTS

This work was supported by grant MGN 1 R55 CA57511-01 from the National Cancer Institute and grant DAMD17-93-J-3044 from the Department of the Army. We thank Roche Molecular Systems for providing us with an XL PCR kit in the early stages of this project. We thank Dr. Ray White and Dr. Ken Ward for providing lymphoblast cell lines prepared from NF1 patients; Mr. Ed Meenen for oligonucleotide syntheses; Ms. Margaret Robertson for sequencing PCR products; and Dr. David Viskochil, Dr. Smita Purandare, Dr. Shun Sawada, and Ms. Shannon Neil for helpful discussions.

The publication costs of this article were defrayed in part by payment of page charges. This article must therefore be hereby marked "advertisement" in accordance with 18 USC section 1734 solely to indicate this fact.

REFERENCES

Andersen, L.B., J.W. Fountain, D.H. Gutmann, S.A. Tarle, T.W. Glover, N.C. Dracopoli, D.E. Housman, and F.S. Collins. 1993. Mutations in the neurofibromatosis 1 gene in sporadic malignant melanoma cell lines. *Nature Genet.* **3:** 118–121.

Barnes, W.M. 1994. PCR amplification of up to 35-kb DNA with high fidelity and high yield from λ bacteriophage templates. *Proc. Natl. Acad. Sci.* **91:** 2216–2220.

Blatt, J., R. Jaffe, M. Deutsch, and J.C. Adkins. 1986. Neurofibromatosis and childhood tumors. *Cancer* **57:** 1225–1229.

Cawthon, R.M., R. Weiss, G. Xu, D. Viskochil, M. Culver, J. Stevens, M. Robertson, D. Dunn, R. Gesteland, P. O'Connell, and R. White. 1990. A major segment of the neurofibromatosis type 1 gene: cDNA sequence, genomic structure, and point mutations. *Cell* **62:** 193–201.

Cheng, S., C. Fockler, W.M. Barnes, and R. Higuchi. 1994. Effective amplification of long targets from cloned inserts and human genomic DNA. *Proc. Natl. Acad. Sci.* **91:** 5695–5699.

Danglot, G., V. Regnier, D. Fauvet, G. Vassal, M. Kujas, and A. Bernheim. 1995. Neurofibromatosis 1 (NF1) mRNAs expressed in the central nervous system are differentially spliced in the 5′ part of the gene. *Hum. Mol. Genet.* **4:** 915–920.

Heim, R.A., L.N. Kam-Morgan, C.G. Binnie, D.D. Corns, M.C. Cayouette, R.A. Farber, A.S. Aylsworth, L.M. Silverman, and M.C. Luce. 1995. Distribution of 13 truncating mutations in the neurofibromatosis 1 gene. *Hum. Mol. Genet.* **4:** 975–981.

Hoffmeyer, S., G. Assum, J. Griesser, D. Kaufmann, P. Nurnberg, and W. Krone. 1995. On unequal allelic expression of the neurofibromin gene in neurofibromatosis type 1. *Hum. Mol. Genet.* **4:** 1267–1272.

Korf, B.R. 1995. *NF1 genetic analysis consortium newsletter.* KORF@A1.TCH.HARVARD.EDU.

Li, Y., G. Bollag, R. Clark, J. Stevens, L. Conroy, D. Fults, K. Ward, E. Friedman, W. Samowitz, M. Robertson, P. Bradley, F. McCormick, R. White, and R. Cawthon. 1992.

Somatic mutations in the neurofibromatosis 1 gene in human tumors. *Cell* **69:** 275–281.

Li, Y., P. O'Connell, H.H. Breidenbach, R. Cawthon, J. Stevens, G. Xu, S. Neil, M. Robertson, R. White, and D. Viskochil. 1995. Genomic organization of the neurofibromatosis 1 gene (NF1). *Genomics* **25:** 9–18.

Nishi, T., P.S.Y. Lee, K. Oka, V.A. Levin, S. Tanase, Y. Morino, and H. Saya. 1991. Differential expression of two types of the neurofibromatosis type 1 (*NF1*) gene transcripts related to neuronal differentiation. *Oncogene* **6:** 1555–1559.

Noronha, C.M.C. 1992. Amplimers with 3′-terminal phosphorothioate linkages resist degradation by *Vent* polymerase and reduce *Taq* polymerase mispriming. *PCR Methods Applic.* **2:** 131–136.

Powell, S.M., G.M. Petersen, A.J. Krush, S. Booker, J. Jen, F.M. Giardiello, S.R. Hamilton, B. Vogelstein, and K.W. Kinzler. 1993. Molecular diagnosis of familial adenomatous polyposis. *N. Engl. J. Med.* **329:** 1982–1987.

Riccardi, V.M. 1992. *Neurofibromatosis: Phenotype, natural history, and pathogenesis*. The Johns Hopkins University Press, Baltimore, MD.

Riccardi, V.M. and J.E. Eichner. 1986. *Neurofibromatosis: Phenotype, natural history, and pathogenesis*. Johns Hopkins University Press, Baltimore, MD.

Roest, P.A.M., R.G. Roberts, S. Sugino, G. van Ommen, and J.T. Dunnen. 1993. Protein truncation test (PTT) for rapid detection of translation-terminating mutations. *Hum. Molec. Genet.* **2:** 1719–1721.

Sarkar, G. and S.S. Sommer. 1989. Access to a messenger RNA sequence or its protein product is not limited by tissue or species specificity. *Science* **244:** 331–334.

Skerra, A. 1992. Phosphorothioate primers improve the amplification of DNA sequences by DNA polymerases with proofreading activity. *Nucleic Acids Res.* **20:** 3551–3554.

Sorensen, S.A., J.J. Mulvihill, and A. Nielsen. 1986. Long-term follow-up of von Recklinghausen neurofibromatosis. Survival and malignant neoplasms. *N. Engl. J. Med.* **314:** 1010–1015.

Takahashi, K., H. Suzuki, T. Kayama, Y. Suzuki, T. Yoshimoto, H. Sasano, and S. Shibahara. 1994. Multiple transcripts of the neurofibromatosis type 1 gene in human brain and in brain tumours. *Clin. Sci.* **87:** 481–485.

The, I., A.E. Murthy, G.E. Hannigan, L.B. Jacoby, A.G. Menon, J.F. Gusella, and A. Bernards. 1993. Neurofibromatosis type 1 gene mutations in neuroblastoma. *Nature Genet.* **3:** 62–66.

Viskochil, D., A.M. Buchberg, G. Xu, R.M. Cawthon, J. Stevens, R.K. Wolff, M. Culver, J.C. Carey, N.G. Copeland, N.A. Jenkins, R. White, and P. O'Connell. 1990. Deletions and a translocation interrupt a cloned gene at the neurofibromatosis type 1 locus. *Cell* **62:** 187–192.

Wallace, M.R., D.A. Marchuk, L.B. Andersen, R. Letcher, H.M. Odeh, A.M. Saulino, J.W. Fountain, A. Brereton, J. Nicholson, A.L. Mitchell, B.H. Brownstein, and F.S. Collins. 1990. Type 1 neurofibromatosis gene: Identification of a large transcript disrupted in three NF1 patients. *Science* **249:** 181–186.

Received October 13, 1995; accepted in revised form December 28, 1995.